Received: 29 April 2023 | Revised: 29 May 2023 | Accepted: 29 May 2023

DOI: 10.14814/phy2.15749

ORIGINAL ARTICLE

The Physiological Society | american physiological society | Physiological Reports

Acute resveratrol exposure does not impact hemodynamics of the fetal sheep

Jack R. T. Darby[1] | **Georgia K. Williams**[2] | **Steven K. S. Cho**[1,3] | **Ashley S. Meakin**[1] | **Stacey L. Holman**[1] | **Megan Quinn**[1] | **Michael D. Wiese**[4] | **Christopher K. Macgowan**[3] | **Mike Seed**[3] | **Janna L. Morrison**[1]

[1]Early Origins of Adult Health Research Group, UniSA: Clinical and Health Sciences, University of South Australia, South Australia, Adelaide, Australia

[2]Preclinical, Imaging and Research Laboratories, South Australian Health and Medical Research Institute, Adelaide, South Australia, Australia

[3]Univeristy of Toronto and The Hospital for Sick Children, Toronto, Ontario, Canada

[4]Centre for Pharmaceutical Innovation, UniSA: Clinical and Health Sciences, University of South Australia, South Australia, Adelaide, Australia

Correspondence
Jack R. T. Darby and Janna L. Morrison, Early Origins of Adult Health Research Group, University of South Australia, GPO Box 2471, Adelaide, SA 5001, Australia.
Email: jack.darby@unisa.edu.au and janna.morrison@unisa.edu.au

Funding information
Australian Research Council, Grant/Award Number: FT170100431 and DP190102263

Abstract

Babies born growth restricted are at an increased risk of both poor short-and long-term outcomes. Current interventions to improve fetal growth are ineffective and do not lower the lifetime risk of poor health status. Maternal resveratrol (RSV) treatment increases uterine artery blood flow, fetal oxygenation, and fetal weight. However, studies suggest that diets high in polyphenols such as RSV may impair fetal hemodynamics. We aimed to characterize the effect of RSV on fetal hemodynamics to further assess its safety as an intervention strategy. Pregnant ewes underwent magnetic resonance imaging (MRI) scans to measure blood flow and oxygenation within the fetal circulation using phase contrast-MRI and T_2 oximetry. Blood flow and oxygenation measures were performed in a basal state and then repeated while the fetus was exposed to RSV. Fetal blood pressure and heart rate were not different between states. RSV did not impact fetal oxygen delivery (DO_2) or consumption (VO_2). Blood flow and oxygen delivery throughout the major vessels of the fetal circulation were not different between basal and RSV states. As such, acute exposure of the fetus to RSV does not directly impact fetal hemodynamics. This strengthens the rationale for the use of RSV as an intervention strategy against fetal growth restriction.

KEYWORDS

cardiovascular, fetal development, fetus, FGR, hemodynamics, IUGR, MRI, PC-MRI, resveratrol, T_2 oximetry

1 | INTRODUCTION

Impaired fetal substrate supply results in fetal growth restriction (FGR; ~10% of all pregnancies), a condition in which the developing fetus does not have a sufficient oxygen and/or nutrient supply to reach its genetically predetermined growth potential (Sharma et al., 2016). While FGR increases the risk of poor short-term outcomes such as preterm delivery and stillbirth (Bukowski et al., 2014), it also predisposes offspring to the development of chronic disease across the life course (Barker et al., 1989; McMillen & Robinson, 2005). As such, there is great interest in the development of intervention strategies that can restore fetal substrate supply to improve outcomes in these complicated pregnancies.

One candidate for intervention in FGR is the polyphenol resveratrol (RSV). RSV has vasodilator properties through its role in enhancing nitric oxide bioactivity by acting as a potent activator of sirtuin-1 (SIRT1). It also has direct antioxidant effects (Hannan et al., 2017); a characteristic that would be beneficial in the setting of FGR where the associated fetal hypoxemia is often accompanied by an increased generation of damaging reactive oxygen species that contribute toward fetal programming of later life chronic disease (Alexander et al., 2015; Giussani et al., 2012; Rueda-Clausen et al., 2012).

We performed a systematic review to better understand both maternal and fetal outcomes from complicated pregnancies where RSV was trialed as an intervention (Darby, Mohd Dollah, et al., 2019). This review identified RSV's ability to improve uterine artery blood flow both in the context of preeclampsia (Poudel et al., 2013) and maternal western diet exposure (Roberts et al., 2014). Importantly, only a handful of studies reported maternal plasma resveratrol concentrations and those that reported the corresponding fetal concentrations did so at only one time point. Given that the timing, severity, and duration of an in utero insult dictates outcomes (Darby, Varcoe, et al., 2020; Morrison, 2008), the same is possible for gestational RSV exposure whereby different ranges of RSV concentrations may yield a variety of outcomes.

Determining the RSV concentrations within the fetal circulation during a maternal RSV intervention is crucial to characterize RSV's potential as an intervention strategy. To address this gap in knowledge, we used the well characterized chronically catheterized pregnant sheep (Morrison et al., 2018). RSV-loaded implants were placed subcutaneously in the pregnant ewe and fetal catheterization surgery was performed to allow for repetitive fetal blood sampling across gestation. Maternal RSV treatment increased uterine artery blood flow, improved fetal oxygenation status, and increased fetal body weight (Darby, Saini, et al., 2019), with no impact on the fetal hemodynamics (Aujla et al., 2021). However, although we detected stable concentrations of RSV within the maternal circulation, we did not detect RSV in fetal plasma, indicating that, unlike rodents (Bourque et al., 2012), nonhuman primates (Roberts et al., 2014), and likely humans, RSV does not cross the sheep placenta. Thus, the chronically catheterized fetal sheep is a unique model in which to tease apart the direct maternal and indirect fetal effects of RSV exposure from the direct fetal effects of RSV exposure.

While RSV may increase nitric oxide production and thus decrease the vascular tone of the fetal cardiovascular system (Xia et al., 2014), there is evidence that polyphenols such as RSV may inhibit prostaglandin synthesis leading to constriction of the ductus arteriosus (DA; Zielinsky & Busato, 2013). During fetal life, blood oxygenation occurs at the placenta with no gas exchange occurring at the fluid filled lungs. The DA allows the majority of right ventricular cardiac output (RVCO) to bypass the pulmonary circulation and flow into the descending aorta (Mielke & Benda, 2001; Prsa et al., 2014; Rudolph, 1985). Although DA closure is necessary at birth when the site of gas exchange shifts from the placenta to the lungs, premature DA constriction in utero is associated with right ventricular dysfunction, fetal hydrops, fetal mortality, and an increased risk of developing neonatal pulmonary hypertension (Enzensberger et al., 2012; Gewillig et al., 2009). Assessing the hemodynamic consequences of fetal RSV exposure is therefore of utmost importance in establishing the safety of RSV as an intervention strategy during the complicated pregnancy.

We have previously validated the use of phase-contrast (PC)-magnetic resonance imaging (MRI) and T_2 oximetry to measure blood flow and oxygen saturation to then calculate oxygen delivery within the circulations of both the human and sheep fetus (Saini et al., 2020). Moreover, the combination of these two clinically relevant MRI techniques has proven useful in understanding the impact that vasoactive compounds have on fetal hemodynamics (Darby, Schrauben, et al., 2020; Dimasi et al., 2021; Duan et al., 2019; Morrison et al., 2022; Saini et al., 2020). Herein, we aimed to utilize these advanced MRI techniques to determine the direct impact that RSV has on the hemodynamics of the fetal sheep. We hypothesized that acute fetal RSV exposure would have no impact on blood flow through the DA.

2 | MATERIALS AND METHODS

2.1 | Ethical considerations

All experimental protocols were reviewed and approved by the Animal Ethics Committee of the South Australian Health and Medical Research Institute (SAHMRI) and abide by the Australian Code of Practice for the Care and Use of Animals for Scientific Purposes developed by the National Health and Medical Research Council. Ewes from the SAHMRI farm (Burra, South Australia) were housed in an indoor facility with a constant ambient temperature of 20–22°C and a 12-h light/dark cycle. Ewes were housed in individual pens in view of other sheep and had ad libitum access to food and water. All investigators understood the ethical principles outlined in Grundy (2015) and the principles of the 3Rs, specifically the reduction of the use of animals in research (Russell & Burch, 1959).

2.2 | Fetal catheterization surgery

At 116–117 days gestational age (GA; term = ~150 days), Merino ewes carrying singleton fetuses (n = 6; 5:1 female:male) underwent surgery under aseptic conditions as previously described (Edwards et al., 1999; Morrison et al., 2001). Anesthesia was induced with intravenous diazepam (0.3 mg/kg) and ketamine (5 mg/kg) and then maintained with isoflurane (1.5%–2.5% in 100% oxygen). Vascular catheters were implanted into the maternal jugular vein, fetal femoral vein, femoral artery, and the amniotic cavity as previously described (Edwards et al., 1999; Morrison et al., 2001). Ewes received an intramuscular injection of antibiotics (3.5 mL of Duplocillin [150 mg/mL procaine penicillin and 112.5 mg/mL benzathine penicillin; Norbrook Laboratories Ltd.]) and 2 mL of 125 mg/mL Dihydrostreptomycin (Sigma-Aldrich) at surgery and for 3 days following surgery. Fetuses received an intramuscular injection of 1 mL of Duplocillin (150 mg/mL procaine penicillin and 112.5 mg/mL benzathine penicillin) and 1 mL of 125 mg/mL Dihydrostreptomycin during surgery. All ewes received an analgesic, meloxicam (0.5 mg/kg, subcutaneously) on the day before surgery and 24 h later (Varcoe et al., 2019). Each fetus received antibiotics (500 mg; sodium ampicillin; Commonwealth Serum Laboratories) intra-amniotically for 4 days post-surgery.

2.3 | Experimental protocol

Pregnant ewes underwent MRI scans between 120 and 124 days GA (e.g., mid-third trimester) after ~16 h of fasting. General anesthesia was induced in the ewe as described for surgery above. The ewe was then positioned on its left side for the duration of the scan and ventilated to ensure normal fetal oxygenation levels (respiratory rate 16–18; ~1 L O_2 and 5 L air). Maternal heart rate and arterial oxygen saturation were measured using an MRI compatible SaO_2/heart rate monitor (Nonin Medical, Inc.). The sensor was placed on the pregnant ewes' teat and measurements were continuously recorded using LabChart 7 (Darby, Saini, et al., 2019; Duan et al., 2019).

The fetal femoral artery and amniotic catheters were connected to displacement transducers, a quad-bridge amplifier and a data acquisition unit (PowerLab; ADInstruments) to record fetal blood pressure (corrected for amniotic pressure). All data were sampled at a rate of 1000 Hz, digitized and recorded using LabChart 7 (ADInstruments). The resulting blood pressure signal acted as a real-time external cardiac trigger for fetal MRI scanning (Duan et al., 2017, 2019; Schrauben et al., 2019).

Imaging was performed on a 3 T clinical MRI system (MAGNETOM Skyra; Siemens Healthineers). Fetal blood flow measurements and oxygen saturations were determined by PC-MRI and T_2 MRI oximetry as previously described (Darby, Schrauben, et al., 2020; Duan et al., 2019; Saini et al., 2020). Measurements were taken in a basal state after a vehicle bolus (50 μL DMSO in 3 mL saline) and then after a bolus dose of RSV (50 μg; Sigma-Aldrich) into the fetal femoral vein. This dose was based on pilot data and set to target fetal RSV plasma concentrations as previously described in fetal nonhuman primates after maternal dietary RSV supplementation (Roberts et al., 2014). MRI acquisition during the RSV state began at 15 min after the RSV bolus was given and lasted ~45 min.

2.4 | Determination of blood flow within the fetal circulation

The fetal femoral arterial pressure waveform was used to generate a cardiac trigger for MRI (Duan et al., 2017; Schrauben et al., 2019). Two-dimensional cine PC imaging was performed to measure blood flow within the fetal circulation with corresponding vessel appropriate velocity encoding (VENC). PC-MRI acquisitions were completed for the ascending aorta (AAo; 150 cm/s), main pulmonary artery (MPA; 150 cm/s), descending aorta (DAo; 150 cm/s), superior vena cava (SVC; 100 cm/s), DA (150 cm/s), left and right pulmonary arteries (LPA/RPA; 80 cm/s), combined carotid arteries (100 cm/s), umbilical vein (UV; 100 cm/s), and ductus venosus (100 cm/s) using the following parameters: flip angle: 30°, repetition time: 7 ms, echo time: 3.18 ms, field of view: 240 mm, in-plane resolution: $1.0 \times 1.0\ mm^2$, slice thickness: 5.0 mm, number of signal averages: 3, and views per segment: 2 according to our previously published technique (Cho et al., 2020; Dimasi et al., 2021; Duan et al., 2019). With ~15 acquired phases in the cardiac cycle, these parameters achieve a temporal resolution of ~28 ms. The typical acquisition time for each vessel was ~2 min. PC cine images were acquired in the short axis plane of the vessels of interest, which were prescribed using two perpendicular long axis views of each vessel. Pulmonary blood flow (PBF) was determined as the sum of blood flow in the LPA and RPA. RVCO was determined as the sum of DA and pulmonary blood flows. Left ventricular output (LVCO) was determined as equal to AAo blood flow and did not include coronary blood flow.

2.5 | Determination of oxygen saturation within the fetal circulation

Due to the paramagnetic properties of deoxyhemoglobin, the T_2 relaxation time of blood is related to the oxygen saturation of blood (Christen et al., 2013). Vessel T_2 oximetry was performed using a T_2-prepared pulse sequence with a balanced steady-state free precession acquisition (Myomaps; Siemens) (Saini et al., 2020; Sun et al., 2015; Xu et al., 2020; Zhu et al., 2016). In-plane resolution was 1.3 × 1.3 mm. MRI acquisition parameters over all subjects and vessels were: repetition time = 4.2 ms, echo time = 2.1 ms, flip angle = 70°, slice thickness = 6 mm, T_2 preparation times = [32, 64, 96, 128, 160, 192] ms, and acquisition time = ~50 s. A non-rigid motion correction algorithm was applied to compensate for slight in-plane fetal movement (co-registration) (Giri et al., 2012).

The T_2 relaxation time for each vessel of interest was analyzed using CVI[42] (Circle Cardiovascular Imaging). The regions-of-interest were manually adjusted for each image slice to cover the central 60% of the vessel of interest (UV, AAo, DAo, MPA, and SVC) (Stainsby & Wright, 1998). Oxygen saturation was then calculated from T_2 relaxation time using the T_2-oxygen saturation relationship for sheep blood as previously described (Saini et al., 2020).

2.6 | Determination of oxygen delivery and consumption

Blood flow and T_2-derived oxygen saturations were combined to calculate overall fetal oxygen delivery (DO_2), fetal oxygen consumption (VO_2), cerebral DO_2, cerebral VO_2, and pulmonary DO_2 using the following equations:

1. Fetal DO_2:

$$DO_2 = 1.36 \times [\mathrm{Hb}] \times Y_{\mathrm{UV}} \times Q_{\mathrm{UV}}$$

2. Cerebral DO_2:

$$DO_2 = 1.36 \times [\mathrm{Hb}] \times Y_{\mathrm{AAo}} \times Q_{\mathrm{CCa}}$$

3. Fetal VO_2:

$$VO_2 = 1.36 \times [\mathrm{Hb}] \times \left(Y_{\mathrm{UV}} - Y_{\mathrm{DAo}}\right) \times Q_{\mathrm{UV}}$$

4. Cerebral VO_2:

$$VO_2 = 1.36 \times [\mathrm{Hb}] \times \left(Y_{\mathrm{AAo}} - Y_{\mathrm{SVC}}\right) \times Q_{\mathrm{CCa}}$$

Q_{UV} represents the measured umbilical vein blood flow; Q_{CCa} represents the combined blood flow of the carotid arteries; Q_{PBF} represents the combined blood flow in the left and right pulmonary arteries; [Hb] represents the mean fetal hemoglobin concentration during MRI scan; 1.36 is the amount of oxygen (mL at one atmosphere) bound per gram of hemoglobin; Y_{UV} represents the oxygen saturation of UV blood; Y_{DAo} represents the oxygen saturation of the DAo blood, Y_{AAo} represents the oxygen saturation of AAo blood, and Y_{SVC} represents the oxygen saturation of the SVC.

2.7 | Blood sampling and fetal blood gas measurements

After fetal surgery, fetal arterial blood samples (0.5 mL) were collected daily to monitor fetal health by measuring the partial pressure of oxygen (PaO_2), partial pressure of carbon dioxide ($PaCO_2$), oxygen saturation (SaO_2), pH, hemoglobin (Hb), hematocrit (Hct), base excess, and lactate concentrations, and the temperature was corrected to 39°C for sheep blood with a RAPIDPOINT 500 (Siemens Healthineers). During the MRI scan, arterial samples (0.5 mL) for fetal blood gas analysis were taken at the beginning and end of each state and blood samples (3 mL) were collected at 15, 45, and 60 min post RSV administration for subsequent RSV plasma concentration analysis.

2.8 | Determination of fetal resveratrol plasma concentrations

Fetal resveratrol plasma concentrations were determined using liquid chromatography–tandem mass spectrometry as per our previously published protocol (Darby, Saini, et al., 2019). Briefly, 100 μL fetal plasma was incubated with 10 μL of 100 ng/mL stable isotope RSV (Resveratrol-13C6; Toronto Research Chemicals) as an internal standard, 80 μL 0.1 M sodium acetate buffer (pH 5.0) and 20 μL β-glucuronidase type HP-2 (50,000 units/L in 0.1 M sodium acetate buffer [pH 5.0]; Sigma, # G7017) in a water bath for 4 h at 37°C. After the incubation period, 1 mL of 100% acetonitrile (Honeywell; #494445) was added and vortexed for a total of 5 min. Samples were centrifuged at 11,000 g for 10 min and the supernatant was removed and evaporate, and the residue was reconstituted in 30% methanol. 25 μL of sample was injected on a Kinetex 1.7 μm F5 LC Column (150 × 2.1 mm; Phenomenex). Mobile phase A was 0.5 mM ammonium fluoride in 5% methanol, and mobile phase B was 0.5 mM ammonium fluoride in 95% methanol. The flow rate was 0.3 mL/min and mobile phase B was initially 30% and increased linearly to 100% at 3.5 min and then held to 4.25 min, after which it was

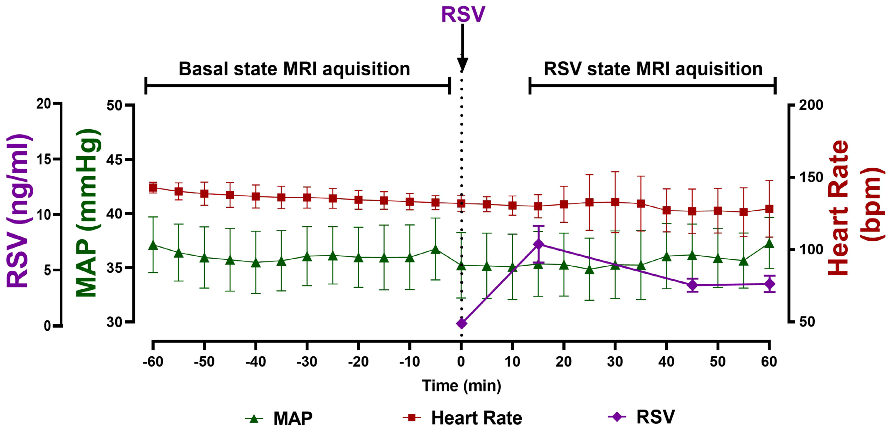

FIGURE 1 Fetal MAP (triangles), HR (squares), and plasma RSV concentrations (diamonds) across the basal and RSV MRI acquisition windows ($n=6$). Data analyzed by a repeated measures one-way ANOVA with a Bonferroni correction for multiple comparisons. Data presented as mean ± SD. $p \le 0.05$. HR, heart rate; MAP, mean arterial pressure; RSV, resveratrol.

TABLE 1 Fetal blood gases, Hb, Hct, and lactate values prior to anesthesia for MRI and during basal and RSV MRI acquisition states.

	Pre-anesthesia ($n=6$)	Basal state ($n=6$)	RSV state ($n=6$)	p-Value
PaO_2 (mmHg)	17.6 ± 1.3^{a}	21.9 ± 2.9^{b}	20.5 ± 3.6^{ab}	0.0209
$PaCO_2$ (mmHg)	49.8 ± 6.3	52.3 ± 6.6	55.4 ± 10.8	0.0834
pH	7.374 ± 0.021^{a}	7.308 ± 0.032^{b}	7.307 ± 0.027^{b}	0.0027
SaO_2 (%)	54.6 ± 7.0	60.8 ± 11.8	57.0 ± 10.5	0.4256
Hb (g/L)	100.2 ± 7.9	96.9 ± 13.9	99.4 ± 13.3	0.4733
Hct (%)	29.7 ± 2.3	28.6 ± 4.2	29.2 ± 3.9	0.4432
Lactate (mmol/L)	1.22 ± 0.17^{a}	2.14 ± 0.40^{b}	2.72 ± 0.51^{b}	0.0028

Note: Values are mean ± SD. Ewes were anesthetized and lying on their left side during MRI. Data analyzed by repeated measures one-way ANOVA with Bonferroni's correction for multiple comparisons. Superscript alphabetical letters indicate significant differences between states ($p < 0.05$) such that values with different alphabetical letters are statistically different from each other and values with the same alphabetical letters are not different.

Abbreviations: Hb, hemoglobin; Hct, hematocrit; MRI, magnetic resonance imaging; $PaCO_2$, partial pressure of carbon dioxide; PaO_2, partial pressure of oxygen; SaO_2, oxygen saturation; RSV, resveratrol.

reduced to 30% at 4.5 min and finally held at 30% B for 6.5 min prior to injection of the next sample. RSV and the stable isotope RSV were detected using a SCIEX 4500 Triple-Quad (SCIEX), which was operated in negative ion mode. Multiple reaction monitoring transitions for RSV and the stable isotope RSV are previously described (Darby, Saini, et al., 2019). Standards were prepared by spiking blank sheep plasma with seven different concentrations of RSV (0.5–40 ng/mL) and were subjected to the same process as above. The ratio of the area of the RSV to internal standard peaks were used to generate standard curves and the concentration of RSV in plasma samples were determined by linear regression.

2.9 | Postmortem

At 123–124 days GA pregnant ewes were humanely killed with an overdose of sodium pentobarbitone (150 mg/kg; Virbac) and the fetus was delivered via hysterotomy and weighed. The fetal body and brain were weighed for blood flow normalization.

2.10 | Statistical analysis

To determine the effect of RSV on fetal blood flow, oxygen delivery, and consumption, a two-tailed paired t-test was used (GraphPad Prism version 8; GraphPad Software). The impact of RSV on fetal blood pressure and heart rate was determined using a repeated measures one-way ANOVA with time (analyzed as 5 min averages every 5 min) as the repeated measure. Based on our previous work using MRI to measure the impact of vasoactive agents on fetal hemodynamics (Darby, Schrauben, et al., 2020), a sample size of $n=6$ is sufficient to achieve 80% power for a paired analysis. Data are presented as mean ± SD and a probability of 5% ($p < 0.05$) was considered significant for all analyses.

3 | RESULTS

3.1 | Fetal plasma RSV concentrations, blood gas, pH, Hb, Hct, and lactate measures

Fetal weight was comparable between fetuses (3.090 ± 0.137; mean ± SD). Following fetal RSV administration, fetal plasma RSV plasma concentrations peaked at 7.13 ± 4.17 ng/mL (mean ± SD) and then remained within the desired range (~5 ng/mL; range = 1.93–5.85 ng/mL) for the duration of the RSV MRI acquisition window (Figure 1).

Fetal $PaCO_2$, SaO_2, Hb, and Hct remained stable from prior to anesthesia and throughout both the basal and RSV acquisition windows. There was no difference in fetal PaO_2 between basal and RSV states. However, fetal PaO_2 was significantly higher (albeit not outside the physiological range for Merino fetal sheep at this GA) during both MRI states than prior to anesthesia (Table 1). There was no difference in fetal pH and lactate between basal and RSV states; however, fetal pH was significantly lower during both MRI states than prior to anesthesia and fetal lactate was significantly higher during both MRI states than prior to anesthesia (Table 1).

3.2 | Impact of RSV on fetal blood pressure and heart rate

There was no impact of RSV exposure on fetal MAP or heart rate compared to the basal state (Figure 1).

3.3 | Impact of RSV on umbilical vein blood flow, ductus venous shunting, fetal oxygen delivery, and consumption

Fetal RSV exposure did not impact umbilical vein blood flow (Figure 2a), the proportion of oxygen-rich blood shunted through the ductus venosus (Figure 2b), overall fetal DO_2 (Figure 2c), or fetal VO_2 (Figure 2d) compared to the basal state.

3.4 | Impact of RSV on blood flow within the fetal circulation

Fetal RSV exposure did not impact RVCO (Figure 3a), pulmonary blood flow (Figure 3c) or blood flow through the DA (Figure 3b). In addition, there was no impact of fetal RSV exposure on blood flow from the right to the left side of the heart through the foramen ovale (Figure 3d), LVCO (Figure 3e), or blood flow to the brain through the carotid arteries (Figure 3f).

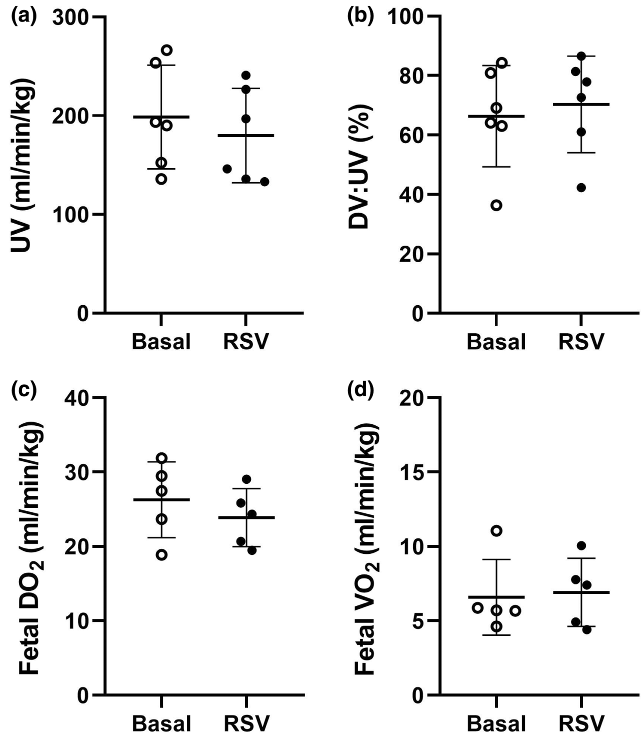

FIGURE 2 Umbilical vein blood flow (a), ductus venous shunting (b), fetal oxygen delivery (c), and fetal oxygen consumption (d) during basal (unfilled circles) and RSV (filled circles) MRI acquisition windows. One animal excluded from fetal DO_2 and VO_2 analysis due to unusable T_2 prescription of the UV (fetal movement). Data analyzed by a paired *t*-test. $p \leq 0.05$. DV, ductus venosus; RSV, resveratrol; UV, umbilical vein.

3.5 | Effect of RSV on cerebral DO_2, cerebral VO_2 and oxygen extraction

Fetal RSV exposure did not impact cerebral DO_2 (Figure 4a), cerebral VO_2 (Figure 4b), or cerebral oxygen extraction fraction (Figure 4c).

3.6 | Effect of RSV on combined ventricular output and blood flow distribution

Combined ventricular output (CVO) was not changed by fetal RSV exposure (Figure 5a). Blood flow distribution (normalized to CVO) throughout the fetal circulation was not changed by fetal RSV exposure (Figure 5b).

4 | DISCUSSION

Maternal RSV treatment has shown great potential as an intervention strategy for FGR in that it increases uterine artery blood flow, improves fetal oxygenation, and

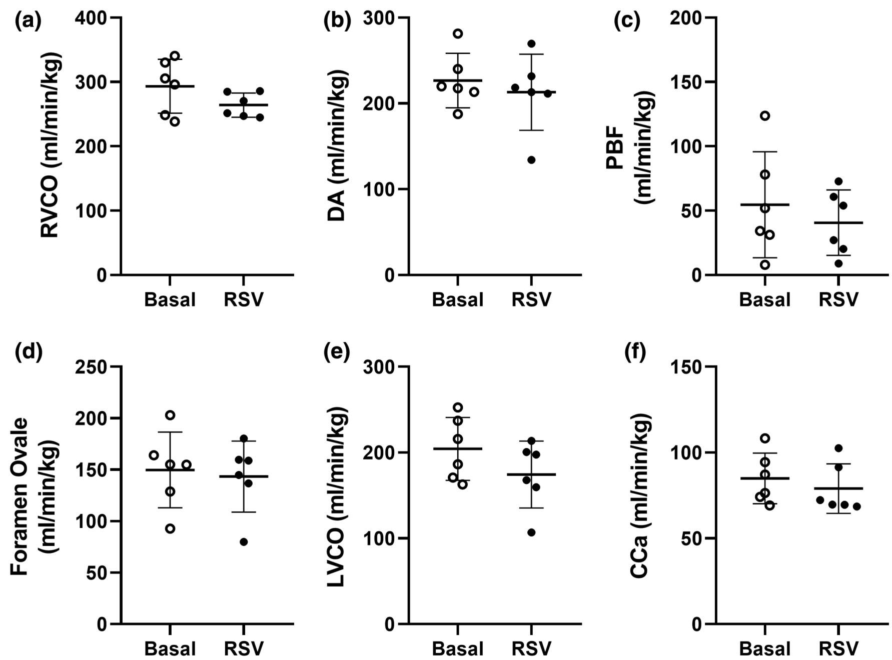

FIGURE 3 Effect of fetal RSV exposure on right ventricular cardiac output [(a) RVCO], blood flow through the ductus arteriosus [(b) DA], pulmonary blood flow [(c) PBF], blood flow through the foramen ovale [(d) FO], left ventricular cardiac output [(e) LVCO], and combined carotid artery blood flow (f). Data presented as individual data points ($n=6$; basal state, unfilled circles; RSV state, filled black circles). Data analyzed by a paired t-test. $p \leq 0.05$. RSV, resveratrol.

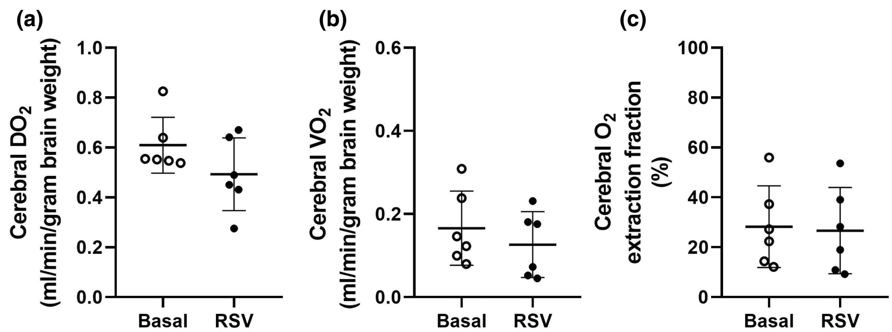

FIGURE 4 Fetal cerebral DO_2 (a), cerebral VO_2 (b), and cerebral oxygen extraction (c) during basal (unfilled circles) and RSV (filled circles) MRI acquisition windows. Data analyzed by a paired t-test. $p \leq 0.05$. MRI, magnetic resonance imaging; RSV, resveratrol.

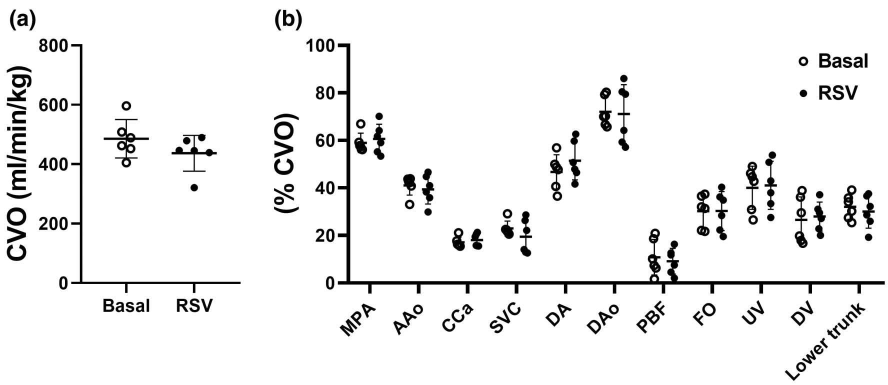

FIGURE 5 Effect of RSV exposure on combined ventricular output [(a) CVO] and blood flow distribution within the fetal circulation (b). Data presented as individual data points ($n=6$; basal state, unfilled circles; RSV state, filled black circles). Data analyzed by a paired t test. $p \leq 0.05$. AAo, ascending aorta; CCa, combined carotid arteries; DA, ductus arteriosus; DAo, descending aorta; DV, ductus venosus; FO, foramen ovale; MPA, main pulmonary artery; PBF, pulmonary blood flow; RSV, resveratrol; SVC, superior vena cava; UV, umbilical vein.

increases fetal body weight (Bourque et al., 2012; Darby, Mohd Dollah, et al., 2019; Darby, Saini, et al., 2019; Lacerda et al., 2023; Poudel et al., 2013; Roberts et al., 2014). However, as a polyphenol there has been concern that through its inhibition of prostaglandin synthesis, RSV may act directly on the fetal vasculature to constrict and close the DA (Zielinsky & Busato, 2013). In such a scenario, there may be adverse fetal cardiovascular complications including right ventricular dilatation, pulmonary volume overload, and tricuspid regurgitation (Bakas et al., 2020; Gewillig et al., 2009). Herein we utilized clinically relevant MRI techniques in combination with the well characterized chronically catheterized pregnant sheep to determine the direct impact that acute RSV exposure has on fetal hemodynamics.

The DA encompasses a thick circumferential muscle layer that allows for effective constriction, ideally at or around the time of birth, when there is a drop in prostaglandins. However, anti-inflammatory mediators such as indomethacin and ibuprofen can cause DA closure through their inhibition of prostaglandin synthesis. For this reason, both are used clinically to treat patent DA in the neonatal period (Ohlsson et al., 2015; Poon, 2007; Thomas et al., 2005). In line with this, the majority of in utero DA closure cases are attributed to maternal ingestion of these drugs. However, there remains a substantial proportion of premature DA closure cases with no definitive etiology. One possible cause of these cases may be maternal ingestion of a diet rich in polyphenols with subsequent fetal exposure. Indeed, polyphenols can inhibit prostaglandin synthesis and may thus have a similar impact on the DA as either ibuprofen or indomethacin (Yoon & Baek, 2005).

Studies in humans have provided substantial evidence that maternal dietary intake of polyphenols is associated with DA constriction and impaired DA flow dynamics (Vian et al., 2018; Zielinsky et al., 2010, 2013; Zielinsky, Piccoli Jr., et al., 2012). Notably, these studies did not report or refer to the exact polyphenol breakdown of the participants' diets. This is important as the term polyphenol encompasses more than 8000 plant compounds with unique structures that are broadly classified as either phenolic acids, flavonoids/flavanols (e.g., cacao, green tea), stilbenes (e.g., RSV), or lignans (Pandey & Rizvi, 2009). To the best of our knowledge, the present study is the first to investigate the impact that a purified form of RSV directly has on fetal DA dynamics. Unlike the aforementioned human studies, we found that fetal RSV exposure had no impact on blood flow through the DA, indicating that RSV may not be the polyphenol responsible DA closure in utero. This notion is supported by preclinical studies that have specifically shown the flavonoids within green tea (Zielinsky, Manica, et al., 2012) and cacao (Zielinsky et al., 2021) are capable of causing premature DA closure and have also demonstrated that alongside prostaglandin inhibition an impairment to fetal NO concentrations by polyphenols may be a key contributor (Bubols et al., 2014). Although, RSV has been shown to inhibit the arachidonic acid pathway and thus the formation of the prostaglandins that aid in keeping the DA patent (Meng et al., 2021), RSV through its potent activation of SIRT-1 is also capable of enhancing NO synthesis (Li & Forstermann, 2009; Milne & Denu, 2008). As such, it is possible that the multifunctional nature of RSV has resulted in the activation of two pathways that have nullified each other's actions on the DA.

Although the literature on premature DA closure following polyphenol exposure directed our focus toward the assessment of DA blood flow, given the vasoactive potential of RSV, a key strength of the present study was our ability to perform a comprehensive analysis on the impact of fetal RSV exposure on blood flow and oxygen delivery throughout the entirety of the fetal circulation. In the context of developing an intervention strategy for use during the complicated pregnancy, the lack of hemodynamic changes that we have found in response to fetal RSV exposure is encouraging as it suggests that RSV at this dose and duration of exposure does not interfere with normal fetal hemodynamics. Importantly, the fetal RSV plasma concentrations under which our hemodynamic assessments were made were similar to those measured in fetal nonhuman primates after a maternal dietary RSV supplementation that increased uterine artery blood flow (Roberts et al., 2014). This implies that the corresponding concentrations of fetal RSV exposure from those maternal concentrations required to have a beneficial impact on utero-placental physiology are hemodynamically safe for the developing fetus.

Although we have shown that fetal RSV exposure does not impact fetal hemodynamics, the duration of RSV exposure used in the present study was acute (~60 min). Should RSV be used clinically as an intervention for FGR, the developing fetus would be chronically exposed to RSV (weeks). Certainly, different durations and gestational timing of RSV exposure have yielded different outcomes across a range of species and pathologies (Darby, Mohd Dollah, et al., 2019; Lacerda et al., 2023). Indeed, RSV's influence on both the activity of eNOS and the prostaglandin synthesis pathway appears to be dependent on the duration of RSV exposure (Takahashi et al., 2000; Wallerath et al., 2002).This raises the question of the impact that a longer more relevant duration of RSV exposure may have on vascular tone, DA patency, and overall fetal hemodynamics. Furthermore, chronic resveratrol exposure has been shown to impact pancreatic development (Roberts et al., 2014) and thus longer term studies would not be restricted to hemodynamic assessments but instead be well placed to further investigate the direct role that resveratrol plays in this pathology as well as development of other fetal organs including the liver, brain, and heart.

Herein, we utilized a combination of advanced MRI techniques to show that not only is the blood flow through the DA not impacted but that normal fetal hemodynamics are preserved during fetal exposure to relevant fetal RSV concentrations. Future studies are warranted to ensure that a more relevant chronic fetal RSV exposure at these same concentrations remains hemodynamically safe for the developing fetus.

AUTHOR CONTRIBUTIONS

Conception or design of the work: Jack R. T. Darby, Christopher K. Macgowan, Mike Seed, and Janna L. Morrison. Acquisition or analysis or interpretation of data for the work: Jack R. T. Darby, Georgia K. Williams, Steven K. S. Cho, Ashley S. Meakin, Stacey L. Holman, Megan Quinn, Michael D. Wiese, Christopher K. Macgowan, Mike Seed, and Janna L. Morrison. Drafting the work or revising it critically for important intellectual content: Jack R. T. Darby, BSS, Stacey L. Holman, Christopher K. Macgowan, Mike Seed, and Janna L. Morrison. Final approval of the version to be published and agreement to be accountable for all aspects of the work: All.

ACKNOWLEDGMENTS

We acknowledge members of the Early Origins of Adult Health Research Group for their expert assistance in surgical procedures and the post-surgical care of the ewe and her fetus. We acknowledge the technical assistance of the National Imaging Facility, a NCRIS capability, at PIRL, SAHMRI. Open access publishing facilitated by University of South Australia, as part of the Wiley - University of South Australia agreement via the Council of Australian University Librarians.

FUNDING INFORMATION

The work was funded by an ARC Discovery Project (DP190102263 to JLM, CKM, MS) and an ARC Future Fellowship (Level 3; FT170100431) to JLM.

CONFLICT OF INTEREST STATEMENT

The authors have no conflicts of interest.

DATA AVAILABILITY STATEMENT

The data that support the findings of this study are available from the corresponding author upon reasonable request.

ETHICS STATEMENT

All experimental protocols were reviewed and approved by the Animal Ethics Committee of the South Australian Health and Medical Research Institute (SAHMRI) and abide by the Australian Code of Practice for the Care and Use of Animals for Scientific Purposes developed by the National Health and Medical Research Council.

ORCID

Jack R. T. Darby https://orcid.org/0000-0001-7114-3920
Georgia K. Williams https://orcid.org/0000-0002-5529-1322
Steven K. S. Cho https://orcid.org/0000-0002-4776-0192
Ashley S. Meakin https://orcid.org/0000-0003-2806-6274
Stacey L. Holman https://orcid.org/0000-0002-6326-4797
Megan Quinn https://orcid.org/0000-0001-9687-4877
Michael D. Wiese https://orcid.org/0000-0002-3255-9242
Christopher K. Macgowan https://orcid.org/0000-0002-7016-0662
Mike Seed https://orcid.org/0000-0001-7330-234X
Janna L. Morrison https://orcid.org/0000-0002-8602-8519

REFERENCES

Alexander, B. T., Dasinger, J. H., & Intapad, S. (2015). Fetal programming and cardiovascular pathology. *Comprehensive Physiology*, *5*, 997–1025.

Aujla, T., Darby, J. R. T., Saini, B. S., Lock, M. C., Holman, S. L., Bradshaw, E. L., Perumal, S. R., McInnes, S. J. P., Voelcker, N. H., Wiese, M. D., Macgowan, C. K., Seed, M., & Morrison, J. L. (2021). Impact of resveratrol-mediated increase in uterine artery blood flow on fetal haemodynamics, blood pressure and oxygenation in sheep. *Experimental Physiology*, *106*, 1166–1180.

Bakas, A. M., Healy, H. M., Bell, K. A., Brown, D. W., Mullen, M., & Scheid, A. (2020). Prenatal duct closure leading to severe pulmonary hypertension in a preterm neonate-a case report. *Cardiovascular Diagnosis and Therapy*, *10*, 1691–1695.

Barker, D. J., Winter, P. D., Osmond, C., Margetts, B., & Simmonds, S. J. (1989). Weight in infancy and death from ischaemic heart disease. *Lancet (London, England)*, *2*, 577–580.

Bourque, S. L., Dolinsky, V. W., Dyck, J. R., & Davidge, S. T. (2012). Maternal resveratrol treatment during pregnancy improves adverse fetal outcomes in a rat model of severe hypoxia. *Placenta*, *33*, 449–452.

Bubols, G. B., Zielinsky, P., Piccoli, A. L., Jr., Nicoloso, L. H., Vian, I., Moro, A. M., Charao, M. F., Brucker, N., Bulcao, R. P., Nascimento, S. N., Baierle, M., Alievi, M. M., Moresco, R. N., Markoski, M., & Garcia, S. C. (2014). Nitric oxide and reactive species are modulated in the polyphenol-induced ductus arteriosus constriction in pregnant sheep. *Prenatal Diagnosis*, *34*, 1268–1276.

Bukowski, R., Hansen, N. I., Willinger, M., Reddy, U. M., Parker, C. B., Pinar, H., Silver, R. M., Dudley, D. J., Stoll, B. J., Saade, G. R., Koch, M. A., Rowland Hogue, C. J., Varner, M. W., Conway, D. L., Coustan, D., Goldenberg, R. L., & Eunice Kennedy Shriver National Institute of Child Health & Human Development Stillbirth Collaborative Research Network. (2014). Fetal growth and risk of stillbirth: A population-based case-control study. *PLoS Medicine*, *11*, e1001633.

Cho, S. K. S., Darby, J. R. T., Saini, B. S., Lock, M. C., Holman, S. L., Lim, J. M., Perumal, S. R., Macgowan, C. K., Morrison, J. L., &

Seed, M. (2020). Feasibility of ventricular volumetry by cardiovascular MRI to assess cardiac function in the fetal sheep. *The Journal of Physiology*, *598*, 2557–2573.

Christen, T., Bolar, D. S., & Zaharchuk, G. (2013). Imaging brain oxygenation with MRI using blood oxygenation approaches: Methods, validation, and clinical applications. *AJNR. American Journal of Neuroradiology*, *34*, 1113–1123.

Darby, J. R. T., Mohd Dollah, M. H. B., Regnault, T. R. H., Williams, M. T., & Morrison, J. L. (2019). Systematic review: Impact of resveratrol exposure during pregnancy on maternal and fetal outcomes in animal models of human pregnancy complications-are we ready for the clinic? *Pharmacological Research: The Official Journal of the Italian Pharmacological Society*, *144*, 264–278.

Darby, J. R. T., Saini, B. S., Soo, J. Y., Lock, M. C., Holman, S. L., Bradshaw, E. L., McInnes, S. J. P., Voelcker, N. H., Macgowan, C. K., Seed, M., Wiese, M. D., & Morrison, J. L. (2019). Subcutaneous maternal resveratrol treatment increases uterine artery blood flow in the pregnant ewe and increases fetal but not cardiac growth. *The Journal of Physiology*, *597*, 5063–5077.

Darby, J. R. T., Schrauben, E. M., Saini, B. S., Holman, S. L., Perumal, S. R., Seed, M., Macgowan, C. K., & Morrison, J. L. (2020a). Umbilical vein infusion of prostaglandin I2 increases ductus venosus shunting of oxygen-rich blood but does not increase cerebral oxygen delivery in the fetal sheep. *The Journal of Physiology*, *598*, 4957–4967.

Darby, J. R. T., Varcoe, T. J., Orgeig, S., & Morrison, J. L. (2020). Cardiorespiratory consequences of intrauterine growth restriction: Influence of timing, severity and duration of hypoxaemia. *Theriogenology*, *150*, 84–95.

Dimasi, C. G., Lazniewska, J., Plush, S. E., Saini, B. S., Holman, S. L., Cho, S. K. S., Wiese, M. D., Sorvina, A., Macgowan, C. K., Seed, M., Brooks, D. A., Morrison, J. L., & Darby, J. R. T. (2021). Redox ratio in the left ventricle of the growth restricted fetus is positively correlated with cardiac output. *Journal of Biophotonics*, *14*, e202100157.

Duan, A. Q., Darby, J. R. T., Soo, J. Y., Lock, M. C., Zhu, M. Y., Flynn, L. V., Perumal, S. R., Macgowan, C. K., Selvanayagam, J. B., Morrison, J. L., & Seed, M. (2019). Feasibility of phase-contrast cine magnetic resonance imaging for measuring blood flow in the sheep fetus. *American Journal of Physiology Regulatory, Integrative and Comparative Physiology*, *317*, R780–R792.

Duan, A. Q., Lock, M. C., Perumal, S. R., Darby, J. R., Soo, J. Y., Selvanayagam, J. B., Macgowan, C. K., Seed, M., & Morrison, J. L. (2017). Feasibility of detecting myocardial infarction in the sheep fetus using late gadolinium enhancement CMR imaging. *Journal of Cardiovascular Magnetic Resonance*, *19*, 69.

Edwards, L. J., Simonetta, G., Owens, J. A., Robinson, J. S., & McMillen, I. C. (1999). Restriction of placental and fetal growth in sheep alters fetal blood pressure responses to angiotensin II and captopril. *The Journal of Physiology*, *515*(Pt 3), 897–904.

Enzensberger, C., Wienhard, J., Weichert, J., Kawecki, A., Degenhardt, J., Vogel, M., & Axt-Fliedner, R. (2012). Idiopathic constriction of the fetal ductus arteriosus: Three cases and review of the literature. *Journal of Ultrasound in Medicine*, *31*, 1285–1291.

Gewillig, M., Brown, S. C., De Catte, L., Debeer, A., Eyskens, B., Cossey, V., Van Schoubroeck, D., Van Hole, C., & Devlieger, R. (2009). Premature foetal closure of the arterial duct: Clinical presentations and outcome. *European Heart Journal*, *30*, 1530–1536.

Giri, S., Shah, S., Xue, H., Chung, Y. C., Pennell, M. L., Guehring, J., Zuehlsdorff, S., Raman, S. V., & Simonetti, O. P. (2012). Myocardial T(2) mapping with respiratory navigator and automatic nonrigid motion correction. *Magnetic Resonance in Medicine*, *68*, 1570–1578.

Giussani, D. A., Camm, E. J., Niu, Y., Richter, H. G., Blanco, C. E., Gottschalk, R., Blake, E. Z., Horder, K. A., Thakor, A. S., Hansell, J. A., Kane, A. D., Wooding, F. B., Cross, C. M., & Herrera, E. A. (2012). Developmental programming of cardiovascular dysfunction by prenatal hypoxia and oxidative stress. *PLoS One*, *7*, e31017.

Grundy, D. (2015). Principles and standards for reporting animal experiments in the journal of physiology and experimental physiology. *The Journal of Physiology*, *593*, 2547–2549.

Hannan, N. J., Brownfoot, F. C., Cannon, P., Deo, M., Beard, S., Nguyen, T. V., Palmer, K. R., Tong, S., & Kaitu'u-Lino, T. J. (2017). Resveratrol inhibits release of soluble fms-like tyrosine kinase (sFlt-1) and soluble endoglin and improves vascular dysfunction - Implications as a preeclampsia treatment. *Scientific Reports*, *7*, 1819.

Lacerda, D. C., Costa, P. C. T., de Oliveira, Y., & de Brito Alves, J. L. (2023). The effect of resveratrol in cardio-metabolic disorders during pregnancy and offspring outcomes: A review. *Journal of Developmental Origins of Health and Disease*, *14*, 3–14.

Li, H., & Forstermann, U. (2009). Resveratrol: A multifunctional compound improving endothelial function. Editorial to: “Resveratrol supplementation gender independently improves endothelial reactivity and suppresses superoxide production in healthy rats” by S. Soylemez et al. *Cardiovascular Drugs and Therapy*, *23*, 425–429.

McMillen, I. C., & Robinson, J. S. (2005). Developmental origins of the metabolic syndrome: Prediction, plasticity, and programming. *Physiological Reviews*, *85*, 571–633.

Meng, T., Xiao, D., Muhammed, A., Deng, J., Chen, L., & He, J. (2021). Anti-inflammatory action and mechanisms of resveratrol. *Molecules*, *26*, 229.

Mielke, G., & Benda, N. (2001). Cardiac output and central distribution of blood flow in the human fetus. *Circulation*, *103*, 1662–1668.

Milne, J. C., & Denu, J. M. (2008). The Sirtuin family: Therapeutic targets to treat diseases of aging. *Current Opinion in Chemical Biology*, *12*, 11–17.

Morrison, J. L. (2008). Sheep models of intrauterine growth restriction: Fetal adaptations and consequences. *Clinical and Experimental Pharmacology & Physiology*, *35*, 730–743.

Morrison, J. L., Berry, M. J., Botting, K. J., Darby, J. R. T., Frasch, M. G., Gatford, K. L., Giussani, D. A., Gray, C. L., Harding, R., Herrera, E. A., Kemp, M. W., Lock, M. C., McMillen, I. C., Moss, T. J., Musk, G. C., Oliver, M. H., Regnault, T. R. H., Roberts, C. T., Soo, J. Y., & Tellam, R. L. (2018). Improving pregnancy outcomes in humans through studies in sheep. *American Journal of Physiology Regulatory, Integrative and Comparative Physiology*, *315*, R1123–R1153.

Morrison, J. L., Chien, C., Gruber, N., Rurak, D., & Riggs, W. (2001). Fetal behavioural state changes following maternal fluoxetine infusion in sheep. *Brain Research. Developmental Brain Research*, *131*, 47–56.

Morrison, J. L., Williams, G. K., Cho, S. K. S., Saini, B. S., Meakin, A. S., Holman, S. L., Quinn, M., Wiese, M. D., Macgowan, C. K., Seed, M., & Darby, J. R. T. (2022). MRI characterization of blood flow and oxygen delivery in the fetal sheep whilst exposed to sildenafil citrate. *Neonatology*, *119*, 1–10.

Ohlsson, A., Walia, R., & Shah, S. S. (2015). Ibuprofen for the treatment of patent ductus arteriosus in preterm or low birth weight (or both) infants. *The Cochrane Database of Systematic Reviews*, *2*, CD003481.

Pandey, K. B., & Rizvi, S. I. (2009). Plant polyphenols as dietary antioxidants in human health and disease. *Oxidative Medicine and Cellular Longevity*, *2*, 270–278.

Poon, G. (2007). Ibuprofen lysine (NeoProfen) for the treatment of patent ductus arteriosus. *Baylor University Medical Center Proceedings*, *20*, 83–85.

Poudel, R., Stanley, J. L., Rueda-Clausen, C. F., Andersson, I. J., Sibley, C. P., Davidge, S. T., & Baker, P. N. (2013). Effects of resveratrol in pregnancy using murine models with reduced blood supply to the uterus. *PLoS One*, *8*, e64401.

Prsa, M., Sun, L., van Amerom, J., Yoo, S. J., Grosse-Wortmann, L., Jaeggi, E., Macgowan, C., & Seed, M. (2014). Reference ranges of blood flow in the major vessels of the normal human fetal circulation at term by phase-contrast magnetic resonance imaging. *Circulation Cardiovascular Imaging*, *7*, 663–670.

Roberts, V. H., Pound, L. D., Thorn, S. R., Gillingham, M. B., Thornburg, K. L., Friedman, J. E., Frias, A. E., & Grove, K. L. (2014). Beneficial and cautionary outcomes of resveratrol supplementation in pregnant nonhuman primates. *FASEB Journal: Official Publication of the Federation of American Societies for Experimental Biology*, *28*, 2466–2477.

Rudolph, A. M. (1985). Distribution and regulation of blood flow in the fetal and neonatal lamb. *Circulation Research*, *57*, 811–821.

Rueda-Clausen, C. F., Morton, J. S., Oudit, G. Y., Kassiri, Z., Jiang, Y., & Davidge, S. T. (2012). Effects of hypoxia-induced intrauterine growth restriction on cardiac siderosis and oxidative stress. *Journal of Developmental Origins of Health and Disease*, *3*, 350–357.

Russell, W. M. S., & Burch, R. L. (1959). *The principles of humane experimental technique*. Methuen.

Saini, B. S., Darby, J. R. T., Portnoy, S., Sun, L., van Amerom, J., Lock, M. C., Soo, J. Y., Holman, S. L., Perumal, S. R., Kingdom, J. C., Sled, J. G., Macgowan, C. K., Morrison, J. L., & Seed, M. (2020). Normal human and sheep fetal vessel oxygen saturations by T2 magnetic resonance imaging. *The Journal of Physiology*, *598*, 3259–3281.

Schrauben, E. M., Saini, B. S., Darby, J. R. T., Soo, J. Y., Lock, M. C., Stirrat, E., Stortz, G., Sled, J. G., Morrison, J. L., Seed, M., & Macgowan, C. K. (2019). Fetal hemodynamics and cardiac streaming assessed by 4D flow cardiovascular magnetic resonance in fetal sheep. *Journal of Cardiovascular Magnetic Resonance*, *21*, 8.

Sharma, D., Shastri, S., & Sharma, P. (2016). Intrauterine growth restriction: Antenatal and postnatal aspects. *Clinical Medicine Insights: Pediatrics*, *10*, 67–83.

Stainsby, J. A., & Wright, G. A. (1998). Partial volume effects on vascular T2 measurements. *Magnetic Resonance in Medicine*, *40*, 494–499.

Sun, L., Macgowan, C. K., Sled, J. G., Yoo, S. J., Manlhiot, C., Porayette, P., Grosse-Wortmann, L., Jaeggi, E., McCrindle, B. W., Kingdom, J., Hickey, E., Miller, S., & Seed, M. (2015). Reduced fetal cerebral oxygen consumption is associated with smaller brain size in fetuses with congenital heart disease. *Circulation*, *131*, 1313–1323.

Takahashi, Y., Roman, C., Chemtob, S., Tse, M. M., Lin, E., Heymann, M. A., & Clyman, R. I. (2000). Cyclooxygenase-2 inhibitors constrict the fetal lamb ductus arteriosus both in vitro and in vivo. *American Journal of Physiology Regulatory, Integrative and Comparative Physiology*, *278*, R1496–R1505.

Thomas, R. L., Parker, G. C., Van Overmeire, B., & Aranda, J. V. (2005). A meta-analysis of ibuprofen versus indomethacin for closure of patent ductus arteriosus. *European Journal of Pediatrics*, *164*, 135–140.

Varcoe, T. J., Darby, J. R. T., Gatford, K. L., Holman, S. L., Cheung, P., Berry, M. J., Wiese, M. D., & Morrison, J. L. (2019). Considerations in selecting postoperative analgesia for pregnant sheep following fetal instrumentation surgery. *Animal Frontiers*, *9*, 60–67.

Vian, I., Zielinsky, P., Zilio, A. M., Schaun, M. I., Brum, C., Lampert, K. V., De Avila, N., Baldissera, G., Klanovicz, T. M., Zenki, K., Zurita-Peralta, J., Olszewski, A., Piccoli, A., Jr., Nicoloso, L. H., Sulis, N., Van Der Sand, L., & Markoski, M. (2018). Increase of prostaglandin E2 in the reversal of fetal ductal constriction after polyphenol restriction. *Ultrasound in Obstetrics & Gynecology: The Official Journal of the International Society of Ultrasound in Obstetrics and Gynecology*, *52*, 617–622.

Wallerath, T., Deckert, G., Ternes, T., Anderson, H., Li, H., Witte, K., & Forstermann, U. (2002). Resveratrol, a polyphenolic phytoalexin present in red wine, enhances expression and activity of endothelial nitric oxide synthase. *Circulation*, *106*, 1652–1658.

Xia, N., Forstermann, U., & Li, H. (2014). Resveratrol and endothelial nitric oxide. *Molecules*, *19*, 16102–16121.

Xu, J., Duan, A. Q., Marini, D., Lim, J. M., Keunen, J., Portnoy, S., Sled, J. G., McCrindle, B. W., Kingdom, J., Macgowan, C. K., & Seed, M. (2020). The utility of MRI for measuring hematocrit in fetal anemia. *American Journal of Obstetrics and Gynecology*, *222*, 81.e1–81.e13.

Yoon, J. H., & Baek, S. J. (2005). Molecular targets of dietary polyphenols with anti-inflammatory properties. *Yonsei Medical Journal*, *46*, 585–596.

Zhu, M. Y., Milligan, N., Keating, S., Windrim, R., Keunen, J., Thakur, V., Ohman, A., Portnoy, S., Sled, J. G., Kelly, E., Yoo, S. J., Gross-Wortmann, L., Jaeggi, E., Macgowan, C. K., Kingdom, J. C., & Seed, M. (2016). The hemodynamics of late-onset intrauterine growth restriction by MRI. *American Journal of Obstetrics and Gynecology*, *214*, 367.e1–367.e17.

Zielinsky, P., & Busato, S. (2013). Prenatal effects of maternal consumption of polyphenol-rich foods in late pregnancy upon fetal ductus arteriosus. *Birth Defects Research Part C, Embryo Today: Reviews*, *99*, 256–274.

Zielinsky, P., Manica, J. L., Piccoli, A. L., Jr., Nicoloso, L. H., Barra, M., Alievi, M. M., Vian, I., Zilio, A., Pizzato, P. E., Silva, J. S., Bender, L. P., Pizzato, M., Menezes, H. S., & Garcia, S. C. (2012). Fetal ductal constriction caused by maternal ingestion of green tea in late pregnancy: An experimental study. *Prenatal Diagnosis*, *32*, 921–926.

Zielinsky, P., Martignoni, F. V., Markoski, M., Zucatti, K. P., Dos Santos, M. G., Pozzobon, G., Magno, P. R., de Bittencourt, A. V., Sulis, N. M., Cardoso, A., Mattos, D., Naujorks, A. A., von Frankenberg, A. D., & Vian, I. (2021). Maternal ingestion of cocoa causes constriction of fetal ductus arteriosus in rats. *Scientific Reports*, *11*, 9929.

Zielinsky, P., Piccoli, A. L., Jr., Manica, J. L., Nicoloso, L. H., Menezes, H., Busato, A., Moraes, M. R., Silva, J., Bender, L., Pizzato, P., Aita, L., Alievi, M., Vian, I., & Almeida, L. (2010). Maternal consumption of polyphenol-rich foods in late pregnancy and fetal ductus arteriosus flow dynamics. *Journal of Perinatology*, *30*, 17–21.

Zielinsky, P., Piccoli, A. L., Jr., Manica, J. L., Nicoloso, L. H., Vian, I., Bender, L., Pizzato, P., Pizzato, M., Swarowsky, F., Barbisan, C., Mello, A., & Garcia, S. C. (2012). Reversal of fetal ductal constriction after maternal restriction of polyphenol-rich foods: An open clinical trial. *Journal of Perinatology*, *32*, 574–579.

Zielinsky, P., Piccoli, A. L., Jr., Vian, I., Zilio, A. M., Naujorks, A. A., Nicoloso, L. H., Barbisan, C. W., Busato, S., Lopes, M., & Klein, C. (2013). Maternal restriction of polyphenols and fetal ductal dynamics in normal pregnancy: An open clinical trial. *Arquivos Brasileiros de Cardiologia*, *101*, 217–225.

How to cite this article: Darby, J. R. T., Williams, G. K., Cho, S. K. S., Meakin, A. S., Holman, S. L., Quinn, M., Wiese, M. D., Macgowan, C. K., Seed, M., & Morrison, J. L. (2023). Acute resveratrol exposure does not impact hemodynamics of the fetal sheep. *Physiological Reports*, *11*, e15749. https://doi.org/10.14814/phy2.15749